

Original articles

Research article

<https://doi.org/10.17308/kcmf.2024.26/11810>

Microstructural and hydrophilic properties of polyethylene terephthalate glycol polymer samples with different 3D printing patterns

A. S. Lenshin, V. E. Frolova✉, S. A. Ivkov, E. P. Domashevskaya

Voronezh State University,
1 Universitetskaya pl., Voronezh 394018, Russian Federation

Abstract

The aim of the work is to study the influence of the 3-D printing process with the Hercules Original printer by sequentially applying polymer layers using the FDM (Fused Deposition Modeling) method on the microstructural and hydrophilic properties of polyethylene terephthalate glycol (PETG) samples with different printing patterns. X-ray phase analysis revealed the presence of a greater ordering of amorphous PETG polymer chains in printed samples, which occurs during thermal and mechanical impact on the initial filamentous sample during 3D printing. This manifests itself in the increase of relative intensity for the main diffraction peak of the amorphous PETG polymer by an order of magnitude for all of the samples with five different print patterns. At the same time, IR spectroscopy data revealed the preservation of all intrastructural chemical bonds of the polymer both in the original thread and in printed samples. Close contact angles of about $\theta \approx 50^\circ$ for all printed samples, which is much smaller than the right angle $\theta = 90^\circ$, show that the surfaces of all five printed PETG samples with different patterns are hydrophilic.

Keywords: Polyethylene terephthalate-glycol PETG, Model drawings 3D printing, X-ray amorphous phase, Ordering of polymer chains, IR spectra, Intrastructural chemical bonds of the polymer, Hydrophilic surface

Funding: The research was carried out with the support of the Ministry of Education and Science of the Russian Federation partly within the framework of the state task for universities in the field of scientific activity, project No. FZGU-2023-006, and Agreement No. 075-15-2021-1351 in parts of the XRD research.

For citation: Lenshin A. S., Frolova V. E., Ivkov S. A., Domashevskaya E. P. Microstructural and hydrophilic properties of polyethylene terephthalate glycol polymer samples with various 3D printing patterns. *Condensed Matter and Interphases*. 2024;26(1): 78–87. <https://doi.org/10.17308/kcmf.2024.26/11810>

Для цитирования: Леньшин А. С., Фролова В. Е., Ивков С. А., Домашевская Э. П. Микроструктурные и гидрофильные свойства образцов полимера полиэтилентерефталат-гликоля с различными рисунками 3D-печати. *Конденсированные среды и межфазные границы*. 2024;26(1): 78–87. <https://doi.org/10.17308/kcmf.2024.26/11810>

✉ Vera E. Frolova, e-mail: ternovaya@phys.vsu.ru

© Lenshin A. S., Frolova V. E., Ivkov S. A., Domashevskaya E. P., 2024



The content is available under Creative Commons Attribution 4.0 License.

1. Introduction

One of the most important tasks of semiconductor microelectronics has always been the creation of high-quality packages for integrated circuits. At present, the manufacture of high-quality and relatively inexpensive packages for integrated circuits from polymers seems to be especially relevant.

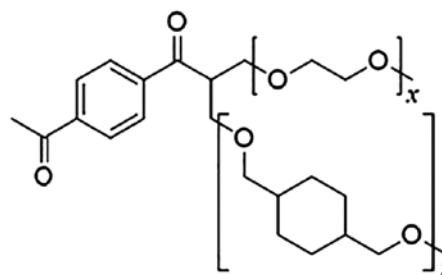
One of these polymers is polyethylene terephthalate glycol PETG (PETG), a high-strength, wear-resistant material with a fairly high melting point (230–240 °C), resistance to most chemicals and ultraviolet radiation. Along with the ease of printing, it has received the widest application in additive manufacturing in the form of threads (filaments) or granules. [1–5]. Glycol-modified PETG polyethylene terephthalate has become a popular material for additive manufacturing and is used, in particular, for printing employing the technology of layer-by-layer imposition of polymer layers by the FDM method (Fused Deposition Modeling) [1]. PETG is an amorphous thermoplastic copolyester [2]. The amorphous nature of PETG is due to the glycol modification of semi-crystalline polyethylene terephthalate (PET). The mechanical characteristics of PETG are similar to those ones of PET [6]. However, PETG is generally regarded as the best polymer for 3D printing. [7]. It is very suitable for extrusion, blow molding, injection molding as well as thermoforming [8]. At the same time, it has excellent chemical resistance, good tensile strength and flexibility [7]. Due to the amorphous structure and relatively strong interlayer bonding, products printed from PETG exhibit a lower anisotropy of mechanical properties compared to other materials manufactured using the FDM technology [8].

In addition, due to its good biocompatibility, it is a suitable material for 3D printing in bone tissue engineering [9].

The dielectric properties of this material make it possible to its widely use in electrical engineering and electronics in the production of cases and elements of electronic devices [10].

PETG is an ideal material for fabricating objects that are subjected to constant loads, systematic shocks or vibrations. PETG is a thermoplastic and is a polycondensation product of ethylene glycol with terephthalic acid (or its dimethyl ester)

with the chemical formula $(C_{10}H_8O_4)_n$. Structural formula of PETG is shown below [2]:



PETG is a solid, colorless, transparent substance in the amorphous state and white, opaque in the crystalline state. It turns into a transparent state when heated to the glass transition temperature (85 °C) and remains in this state when it is abruptly cooled and quickly passes through the “crystallization zone”. One of the important parameters of PETG is the intrinsic viscosity, which is determined by the length of the polymer molecule. As the intrinsic viscosity increases, the rate of crystallization decreases. PETG can be dyed, metallized, and printed.

The aim of this work is to study the effect of 3D printing of polyethylene terephthalate glycol (PETG) samples with different model patterns on their microstructural properties and surface wettability.

2. Experimental

Objects and methods of research. The samples for the study were made from a polyethylene terephthalate glycol PETG filament with a diameter of 1.75 mm employing Hercules Original 3D printer by layer-by-layer superposition of FDM polymer layers (Fused Deposition Modeling) [1]. Extruder temperature – 260 °C, power – 500 W. 5 cylindrical specimens with a diameter of 20 mm and a thickness of 5 mm were printed. The printed samples differed in 3D printing patterns (five model types).

Figure 1 shows the studied types of model drawings.

Along with the printed samples, the original filamentous PETG sample (Filament) was studied. Therefore, in the next section of the article, the results of the study of microstructural properties for six samples will be presented.

X-ray phase analysis (XRD) of all the above PETG samples was carried out with DRON-4.07

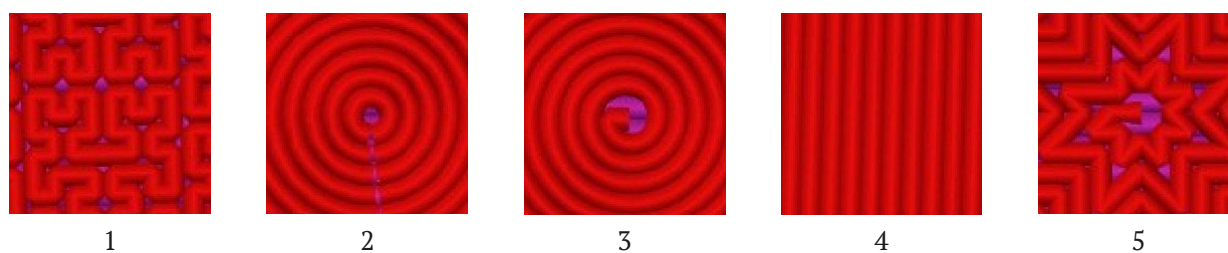


Fig. 1. Five types of 3-D printing patterns on polyethylene terephthalate glycol (PETG) polymer samples: 1_Hilbert, 2_Concentric, 3_Archimedean, 4_Rectilinear, 5_Octagram

diffractometer with $\text{CuK}\alpha$ - radiation in the step-by-step scanning mode applying sample rotation, with copper radiation $\text{CuK}\alpha$ $\lambda = 1.54 \text{ \AA}$ at high voltage and filament current of the X-ray tube anode $U = 29 \text{ kV}$ and $I = 25 \text{ mA}$.

The measurements of small-angle X-ray diffraction of the samples were carried out at the Central Collective Use Center of the NO VSU on an ARLX'TRA diffractometer in parallel beam geometry and the θ - θ mode in the angle range $2\theta = 1$ - 10° using $\text{CuK}\alpha_1$ radiation with the use of a monochromator.

IR spectroscopy is a universal method for obtaining information about the molecular structure of substances and allows to determine the nature of atomic groups, the nature of chemical bonds and their changes under the influence of external conditions. Any molecule has its own individual spectrum of vibrations; therefore, by comparing the modes of the obtained experimental spectrum with the known literature data, it is possible to identify the substance under study. Studies of the molecular structure of PETG samples were carried out on five 3D printed samples with different model

patterns (Fig. 1) and the original filament by measuring IR transmission spectra using the ATR (attenuated total internal reflection) method on a Bruker Vertex 70 IR-Fourier spectrometer of the Center for Collective Use of the Voronezh State University.

The wettability studies of the surface of flat printed samples with various 3D printed model patterns (Fig. 1) were carried out with a setup for measuring contact angles (Fig. 2), which we made with 3D printer. The setup is a stand with a sample holder on which a flat sample is placed. A drop-meter is installed on top, with the help of which drops are created on the surface of the sample to measure the contact angle of wetting. Opposite the stand with the test sample, a webcam is installed, which displays the image of the drop on the screen, and using the Pic-pic graphics editor, the wetting angle of the sample θ is measured. A drop of liquid on the surface of a solid, depending on the nature of the solid, the liquid and the environment in which it is located, can spread completely or partially and take the form shown in Fig. 3. The angle θ between the tangent to the surface of the drop and the surface



Fig. 2. Installation for measuring contact angles

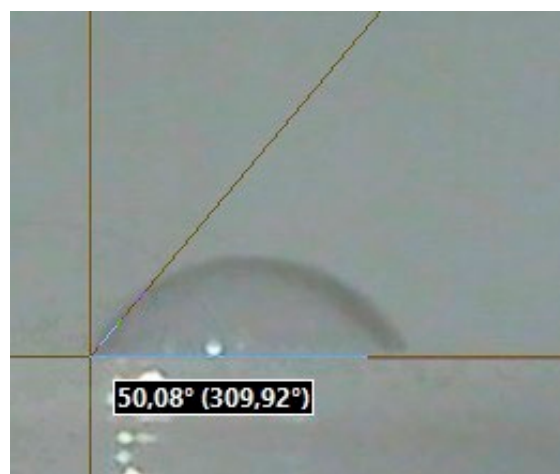


Fig. 3. Contact angle ϕ on a hydrophilic surface

of the solid, counted towards the droplet surface is called the contact angle θ [9, 10].

If a liquid drop completely or partially spreads over the sample surface and forms an acute angle $\varphi < 90^\circ$ with it, as is shown in Fig. 3, then the liquid wets this surface. Only those liquids can moisten a solid surface that have lower the surface tension than a given solid at the boundary with air. Surfaces of solids wetted by water are called *hydrophilic*. Surfaces where water does not spread and forms an obtuse contact angle $\varphi > 90^\circ$ are called *hydrophobic*.

3. Results and discussion

3.1. X-ray phase analysis of PETG samples

Fig. 4 shows the results of analyzing the crystalline state of the samples under study with 5 different 3D printing patterns, 1_Hilbert, 2_Concentric, 3_Archimedian, 4_Rectilinear, 5_Octogram, and the original filament (Filament) by X-ray methods in two intervals of Bragg angles: small angles $2\theta = 1-10^\circ$ (upper Fig. 4 a) and large angles $2\theta = 10-90^\circ$ (lower Fig. 4b).

The obtained results show that at small angles, all of the studied samples do not give

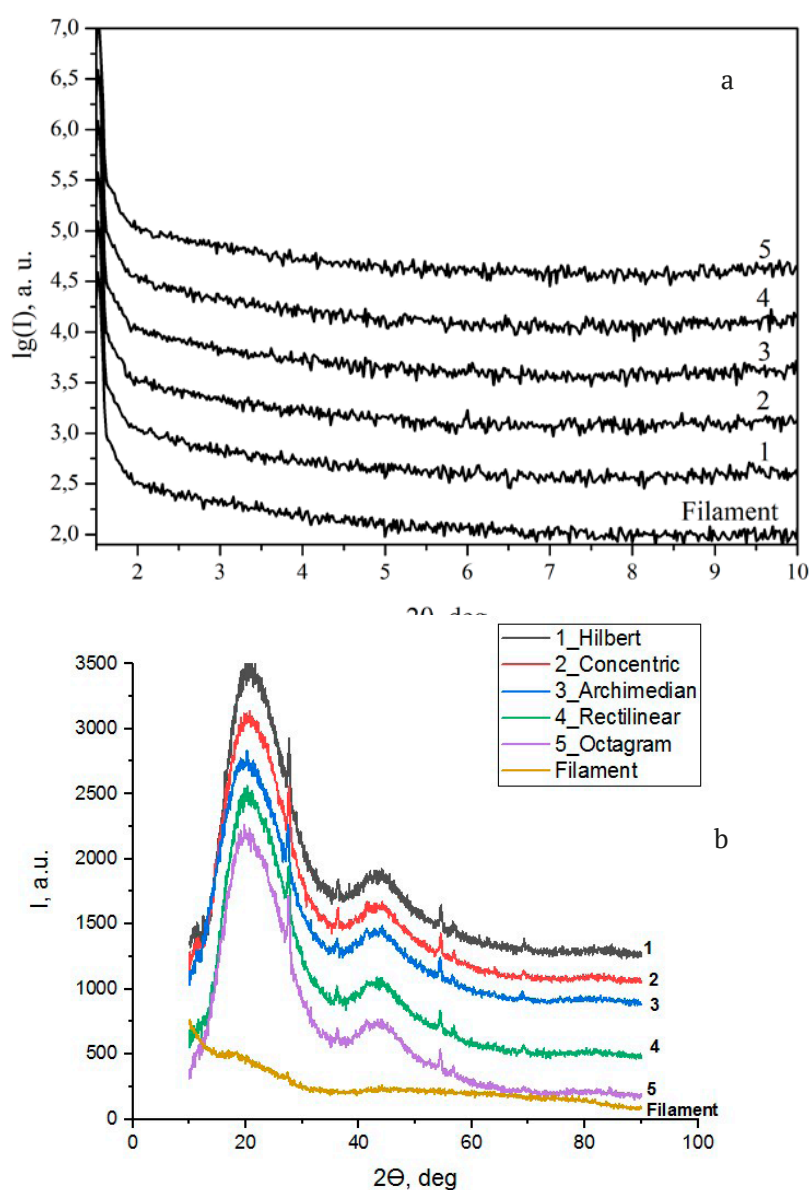


Fig. 4. Diffraction patterns of samples with model patterns 1_Hilbert, 2_Concentric, 3_Archimedian, 4_Rectilinear, 5_Octogram and the original filament for 3D printing (Filament) in two intervals of Bragg angles: small angles $2\theta = 1-10^\circ$ (upper Fig. 4a) and large angles $2\theta = 10-90^\circ$ (lower Fig. 4b)

any reflections (Fig. 4a), while in the range of large angles, the diffraction patterns of all 5 printed samples with different patterns contain two wide reflections (halos) from the amorphous phase of PETG with the most intense reflection in the range of angles $2\theta \approx 15\text{--}35^\circ$ and the second less intense in the range $2\theta \approx 37\text{--}55^\circ$ (Fig. 4b). Against the background of these wide bands, all five printed samples show narrow diffraction lines from the crystalline phase of the coloring pigment of the PETG polymer [11], which is titanium dioxide TiO_2 with a tetragonal rutile structure [11, 12].

At the same time, in the diffraction pattern of the original filament (6_Filament, Fig. 4b), the intensity of the first halo with a maximum at $2\theta \approx 20^\circ$ decreases by an order of magnitude, and the second halo is stretched two to three times in the 2θ scale, as compared to all printed samples. And against the background of the first halo of the original thread, only a trace is outlined from one of the most intense lines of the TiO_2 (110) pigment. Such differences in the diffraction patterns of the printed samples from the diffraction pattern of the original thread are due to greater order in the orientation of the rigid polymer chains of amorphous PETG in the printed samples with different patterns, which occurs in the extruder under thermal and mechanical influences on the original thread-like sample during the 3D printing process. However, it should be noted that the characteristic amorphous structure of filamentary PETG samples from different manufacturers used for 3D printing may differ in the degree of ordering of polymer chains, which is reflected in the intensity of the first halo of the diffraction patterns of the initial filaments.

Nevertheless, in [11], when studying the effect of various 3D printing speeds on the microstructure, morphology and mechanical properties of the printed samples $20 \times 20 \times 3$ mm in size, a PETG (filament) thread with a diameter of 1.75 mm, manufactured by FUEL INVEST, SE, Prague, Czech Republic, was used, and its diffraction pattern, in fact, did not differ from those ones of the printed samples with different printing speeds as well as our samples with different patterns. However, the differences observed in the diffraction pattern of the relative intensity of the first halo of our original filament

(Filament) in Fig. 4b from the original filament of work [11] may be due to the peculiarities of the technology of the manufacturer of filaments (Filaments) for 3D printing.

Table 1 shows the values of the Bragg angles 2θ and interplanar distances d of the TiO_2 crystalline pigment in the printed PETG samples, related by Wolfe–Bragg formula:

$$2d \cdot \sin \theta = n \cdot \lambda,$$

where n – is the order of reflection, λ is the wavelength of X-ray radiation $\text{CuK}\alpha$ $\lambda = 1.54 \text{ \AA}$.

Analysis of the interplanar distances d_{hkl} of the crystalline phase of the TiO_2 pigment shows that these values, measured in angstroms $1 \text{ \AA} = 10^{-10} \text{ m}$, are almost the same for all five samples (with an accuracy to the second decimal places) and are close to the values from the database [11]. This fact, together with the preservation of the relative intensities of the diffraction lines against the background of unchanged intense halos from the amorphous PETG phase of the printed samples, means that the initial filamentous PETG polymer experiences the same thermal and mechanical effects during layer-by-layer deposition by an extruder on a flat surface of any pattern out of the five studied samples.

3.2. IR spectra of PETG samples

IR spectroscopy is a non-destructive optical method used to solve specific problems, including the determination of the fundamental characteristics of a molecule, the quantitative analysis of the known phases in a substance, the identification of chemical compounds and the elucidation of their structure. This optical method is based on the measurement of intensity of the infrared (IR) radiation absorbed or reflected by a certain material, which is associated with vibrational and rotational vibrations of molecular fragments and manifests itself in the distribution of intensity in absorption bands depending on the wavelength (λ) or its reciprocal value, which known as the wavenumber (ν).

Fig. 5 shows the IR transmission spectra for the original filament (PETG filament) and five 3D printed samples with different PETG polymer patterns.

Table 2 shows the vibrational modes of the IR spectra for all six samples. In the last column of the table, for comparison, the vibrational modes

Table 1. Bragg angles 2θ and interplanar distances d (Å) of most intense lines of the TiO_2 pigment tetragonal phase in printed PETG samples with different model patterns

Printed Sample PETG	2θ , (°)	d_{hkl} (Å)	d_{hkl} of tetragonal rutile structure TiO_2 [11]
1_Hilbert	27.70	3.222	3.247 (110)
	36.50	2.464	2.487 (101)
	54.65	1.681	1.687 (211)
	56.65	1.628	1.623 (220)
	69.40	1.356	1.359 (301)
2_Concentric	28.0	3.201	3.247 (110)
	36.15	2.489	2.487 (101)
	54.65	1.681	1.687 (211)
	56.85	1.621	1.623 (220)
	69.35	1.356	1.359 (301)
3_Archimedian	27.30	3.269	3.247 (110)
	36.0	2.497	2.487 (101)
	54.50	1.685	1.687 (211)
	56.80	1.621	1.623 (220)
	69.05	1.360	1.359 (301)
4_Rectilinear	27.45	3.256	3.247 (110)
	36.25	2.481	2.487 (101)
	54.55	1,685	1.687 (211)
	56.55	1.628	1.623 (220)
	69.25	1.358	1.359 (301)
5_Octilinear	27.65	3.229	3.247 (110)
	36.05	2.497	2.487 (101)
	54.65	1.681	1.687 (211)
	56.75	1.624	1.623 (220)
	69.55	1.353	1.359 (301)

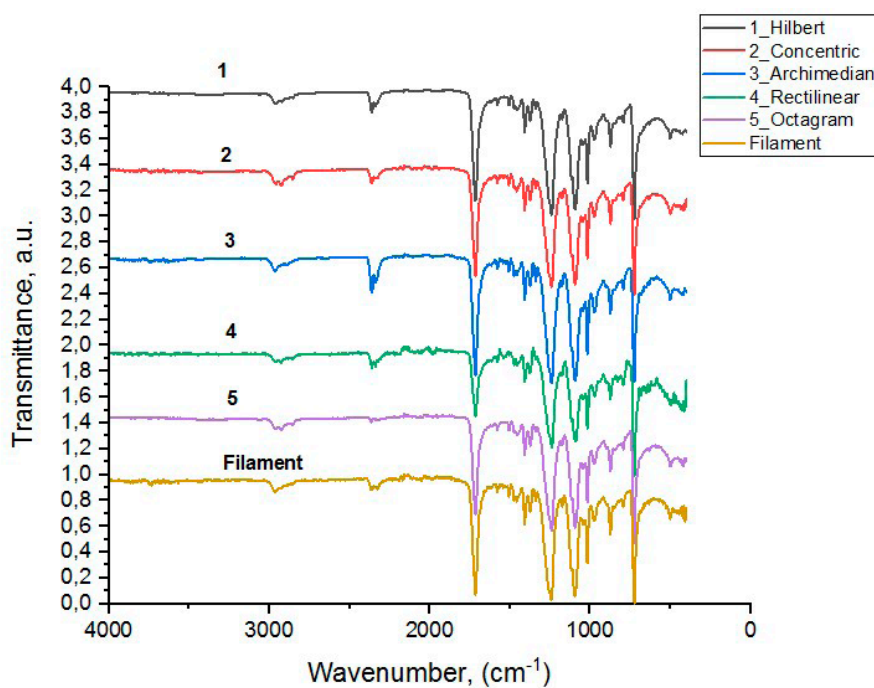
**Fig. 5.** IR transmission spectra for the original sample of PETG thread and five samples with different model patterns of 3D printing from PETG polymer

Table 2. Vibration modes of the IR spectra of the original filament and PETG polymer samples with different 3D printing model patterns in comparison with the literature data for PET (PET) [15]

Identification of vibration modes	Vibration modes of samples PETG, cm ⁻¹						
	Original filament	1_Hilbert	2_Concentric	3_Archimedean	4_Rectilinear	5_Octagram	Modes of PET
Interaction of polar ester groups with benzene rings	723	723	723	725	723	723	712
Vibrations of neighboring aromatic protons in <i>para</i> -substituted aromatic rings	792	790 1978	791 1965	797 1965	791 1975	795 1987	795 1960
1,2,4,5-tetrasubstituted benzene rings	871 972	875 974	872 968	876 968	874 975	872 972	872 972
Methylene group and C-O ester bond vibrations	1043 1093	1043 1093	1043 1094	1047 1096	1045 1092	1043 1094	1050 1096
Terephthalate group (OCC ₆ H ₄ -HCOO)	– 1238	1112 1244	1114 1244	– 1234	1116 1238	1116 1240	1124 1240
Stretching vibrations of C-O in the C-O-H fragment of ethylene glycol and bending vibrations of this segment	1406 1460	1407 1454	1408 1458	1406 1458	1406 1458	1407 1454	1410 1453
Vibrations of the aromatic framework with bond stretching C=C	1504 1575	1506 1577	1506 1577	1535 1574	1502 1578	1502 1576	1504 1577
Stretching of the C=O carboxyl group	1716	1714	1713	1716	1717	1717	1730
Symmetrical stretching of the C-H bond	2918 2952	2922 2964 3068	– 2954 3051	2932 2955 –	2928 2966 3049	2922 2961 3060	2908 2969 3054

of the polyethylene terephthalate polymer PET (PET) from [13] are presented.

The results of IR spectroscopy show that the wave numbers and relative intensities of the vibration modes of all five printed samples with different patterns have almost the same values and coincide within the measurement accuracy with the corresponding values of the fundamental modes of the original PETG filament used in 3D printing of the samples and the literature data for PET polymer modes [12]. This means that the intramolecular chemical bonds of the PETG polymer are not subjected to mechanical and thermal influences during the 3D printing process. These effects impact only on the degree of ordering of polymer chains and they are manifested in a change in the relative intensity of the main diffraction maximum of the amorphous PETG polymer in the printed samples compared to the original thread, observed in Fig. 4b.

3.3. Wettability of the surface of printed samples with different model patterns

The wettability of a solid surface is a manifestation of intermolecular interaction at the contact boundary of three phases: solid, liquid and gas, which is expressed in the spreading of a liquid over the surface of a solid. Since the measurement of the contact angle of surface wetting is carried out only for the flat samples, this section presents the results of the study of wettability for only five printed samples. Fig. 6 shows the screen images of the setup for measuring the wetting angle of drops on the surface of five samples with different 3D printing patterns from PETG polymer.

Measurements of contact angles were carried out at five points of each sample, and in table 3 shows the average values of these angles.

A comparative analysis of the values of the contact angles of wetting shows that they all deviate only slightly from the angle $\varphi \approx 50^\circ$. And only one sample with pattern 1_Hilbert shows an

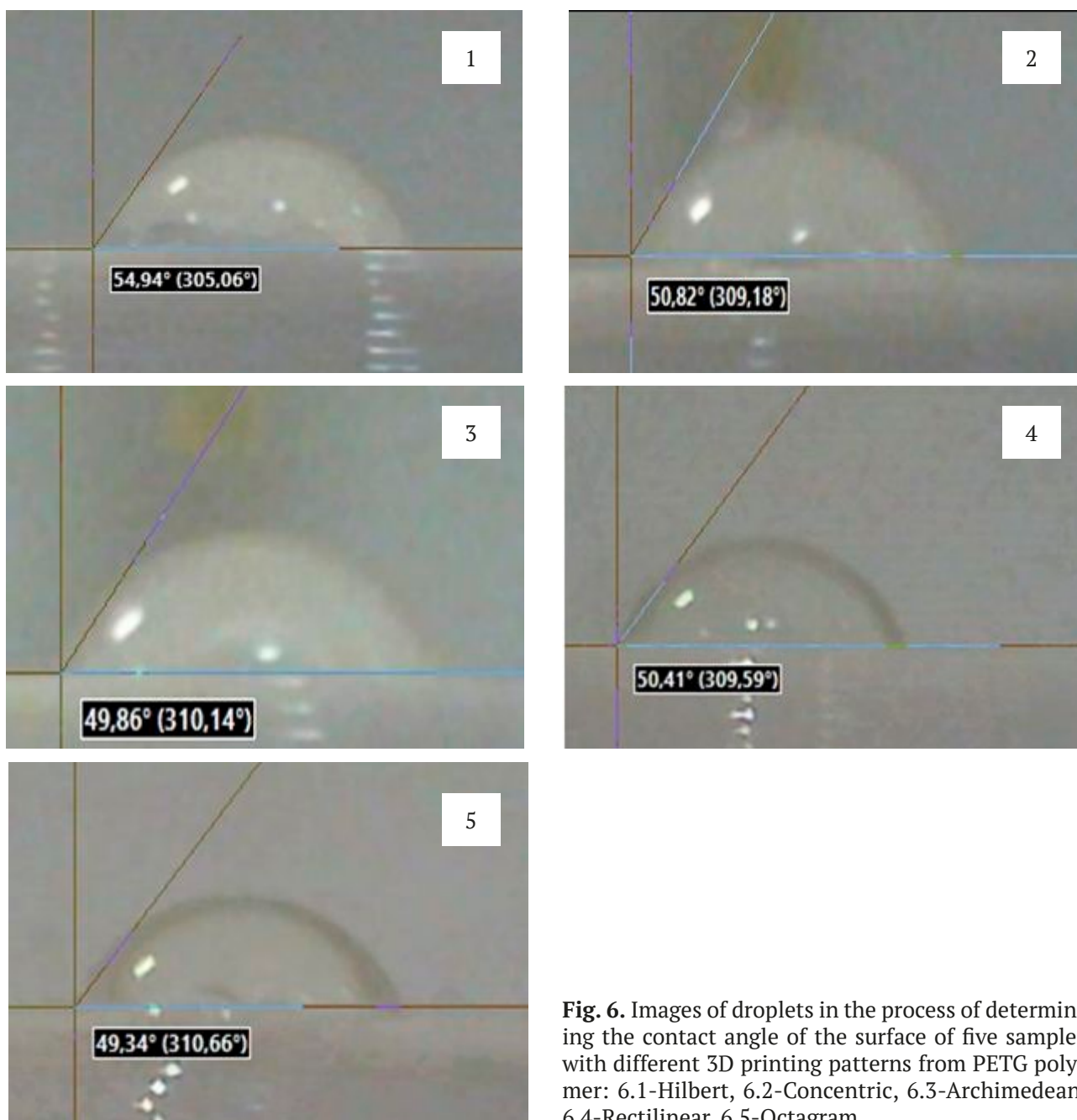


Fig. 6. Images of droplets in the process of determining the contact angle of the surface of five samples with different 3D printing patterns from PETG polymer: 6.1-Hilbert, 6.2-Concentric, 6.3-Archimedean, 6.4-Rectilinear, 6.5-Octagram

Table 3. Average contact angles of the surface of PETG polymer samples with different 3D printing patterns

Type of model pattern when 3D printing a sample	Average contact angle φ , degree
1_Hilbert	52.84
2_Concentric	50.55
3_Archimedean	49.54
4_Rectilinear	50.10
5_Octagram	50.03

average contact angle $\varphi = 52.84$, which is slightly higher than the corresponding values for samples with other patterns by one or two degrees, i.e. by an amount within the accuracy of determining the contact angle.

However, the result of a large deviation of the average value of the contact angle $\varphi \approx 50^\circ$ for all five samples with respect to the right angle of 90° shows that the surfaces of all printed samples with different patterns are hydrophilic, i.e. wettable.

And since the wettability of the surface of a solid body is a manifestation of intermolecular interactions at the interface of contact of the liquid with the surface of the solid body, it should be assumed that one of the mechanisms of such interaction may be the participation of polar ester groups of the PETG polymer in the formation of hydrogen bonds with water molecules on the surface of all five samples, leading to a significant decrease in contact angles relative to 90° .

4. Conclusion

The results obtained in the study of the effect of 3D printing process by successively applying polymer layers employing FDM (Fused Deposition Modeling) method with the Hercules Original 3D printer at an extruder temperature of 260°C and a power of 500 W on the microstructural and hydrophilic properties of polyethylene terephthalate glycol (PETG) samples with different drawings, X-ray diffraction analysis, IR spectroscopy and measurement of the wetting angle showed that:

- differences between the diffraction patterns of printed samples and the diffraction pattern of the original thread are due to the greater ordering of the polymer chains of amorphous PETG in samples with different patterns, which occurs under thermal and mechanical effects on the original filamentous sample during 3D printing and manifests itself in an increase by an order of magnitude in the relative intensity of the main diffraction maximum of amorphous PETG polymer in printed samples;

- at the same time, the intrastuctural chemical bonds of the PETG polymer are not subjected to the effects of 3D printing process, and therefore the wave numbers and relative intensities of the vibration modes of all five printed samples with different patterns have almost the same values and coincide within the measurement accuracy with the corresponding values of the fundamental modes of the original thread PETG used in 3D printing of samples;

- contact angles for all printed samples show close values to the value of $\theta \approx 50^\circ$, which is much smaller than the right angle $\theta = 90^\circ$, show that the surfaces of all five printed PETG samples with different patterns are hydrophilic.

- one of the mechanisms of intermolecular interaction at the interface of a drop of water with the surface of printed samples may be the participation of polar ester groups of the PETG polymer in the formation of hydrogen bonds with water molecules on the surface of all five samples, leading to a significant decrease in contact angles relative to 90° .

Thus, according to the results of our study, PETG has asserted itself as a material suitable for 3D printing using a common printer model. At the same time, 3D printing causes statistically significant orientation of polymer chains in the amorphous PETG material, which is all the same for all five patterns, as a result of extrusion-induced molecular alignment, without destroying the intrastuctural chemical bonds of the polymer.

The declared contribution of the authors

All authors have made an equivalent contribution to the preparation of the publication

Conflict of interest

The authors state that they have no known financial conflicts, interests or personal relationships that could affect the work presented in this article.

References

1. Vidakis N., Petousis M., Velidakis E., Liebscher M., Mechtcherine V., Tzounis L. On the strain rate sensitivity of fused filament fabrication (FFF) processed PLA, ABS, PETG, PA6, and PP thermoplastic polymers. *Polymers*. 2022;12: 2924. <https://doi.org/10.3390/polym12122924>
2. Silva A. L., Salvador G. M. da S., Castro S. V. F., Carvalho N. M. F., Munoz R. A. A. 3D printer guide for the development and application of electrochemical cells and devices. *Frontiers in Chemistry*. 2021;9: 684256. <https://doi.org/10.3389/fchem.2021.684256>
3. Vidakis N., Petousis M., Tzounis L., ... Mountakis N. Sustainable additive manufacturing: mechanical response of polyethylene terephthalate glycol over multiple recycling processes. *Materials*. 2021;14: 1162. <https://doi.org/10.3390/ma14051162>
4. Gordeev E. G., Ananikov V. P. Widely accessible 3D printing technologies in chemistry, biochemistry and pharmaceuticals: applications, materials and prospects. *Russian Chemical Reviews*. 2020;89(12): 1507–1561. <https://doi.org/10.1070/rcr4980>

5. Bex G. J. P., Ingenhuth B. L. J., Cate T., Sezen M., Ozkoc G. Sustainable approach to produce 3D-printed continuous carbon fiber composites: A comparison of virgin and recycled PETG. *Polymer Composites*. 2021;42: 4253–4264. <https://doi.org/10.1002/pc.26143>

6. Schneevogt H., Stelzner K., Yilmaz B., Abali B. E., Klunker A., Völlmecke C. Sustainability in additive manufacturing: exploring the mechanical potential of recycled PET filaments. *Composites and Advanced Materials*. 2021;30: 263498. <https://doi.org/10.1177/26349833211000063>

7. Latko-Durałek P., Dydek K., Boczkowska A. Thermal, rheological and mechanical properties of PETG/rPETG blends. *Journal of Polymers and the Environment*. 2019;27(11): 2600–2606. <https://doi.org/10.1007/s10924-019-01544-6>

8. Dolzyk G., Jung S. Tensile and fatigue analysis of 3D-printed polyethylene terephthalate glycol. *Journal of Failure Analysis and Prevention*. 2019;19: 511. <https://doi.org/10.1007/s11668-019-00631-z>

9. Hassan M. H., Omar A. M., Daskalakis E., ... B'artolo P. The potential of polyethylene terephthalate glycol as biomaterial for bone tissue engineering. *Polymers*. 2020;12: 3045. <https://doi.org/10.3390/polym12123045>

10. Sobolev D. I., Proyavin M. D., Parshin V. V., Belousov V. I., Ryabov A. V. Broadband, low-reflection microwave windows manufactured using 3D printing*. In: *X All-Russian Scientific and Technical Conference "Microwave Electronics and Microelectronics". Collection of reports. Saint-Petersburg, 31 of May – 4 of June, 2021. Saint Petersburg*. St. Petersburg: St. Petersburg State Electrotechnical University "LETI" Publ.; 2021. p. 52. (In Russ.)

11. Kiselev M. G., Savich V. V., Pavich T. P. Determination of contact wetting angle on flat surfaces. *Vestnik BNTU*. 2006;1: 38. (In Russ., abstract in Eng.). Available at: <https://www.elibrary.ru/item.asp?id=21398120>

12. Elesina V. V. *Contact angle. Guidelines*. Altai State Technical University named after. I. I. Polzunov Publ.; 2019: 22. (In Russ.)

13. Loskot J., Jezbera D., Bušovský D., ... Zubko M. Influence of print speed on the microstructure, morphology, and mechanical properties of 3D-printed PETG products. *Polymer Testing*. 2023;123: 108055. <https://doi.org/10.1016/j.polymertesting.2023.108055>

14. ICDD Card: 04-003-0648 tetragonal TiO₂

15. Pereira A. P. dos S., da Silva M. H. P., Júnior É. P. L., Paula A. dos S., Tommasini F. J. Processing and characterization of PET composites reinforced with geopolymer concrete waste. *Materials Research*. 2017;20(suppl 2): 411–420. <https://doi.org/10.1590/1980-5373-mr-2017-0734>

Information about the authors

Alexander S. Lenshin, Dr. Sci. (Phys.–Math.), Leading Researcher, Department of Solid State Physics and Nanostructures, Voronezh State University (Voronezh, Russian Federation).

<https://orcid.org/0000-0002-1939-253X>
lenshinas@mail.ru

Vera E. Frolova, Cand. Sci. (Phys.–Math.), Senior Lecturer, Department of Solid State Physics and Nanostructures, Voronezh State University (Voronezh, Russian Federation).

<https://orcid.org/0009-0000-2880-8958>
ternovaya@phys.vsu.ru

Sergey S. Ivkov, Cand. Sci. (Phys.–Math.), Senior Electronics Engineer, Department of Solid State Physics and Nanostructures, Voronezh State University (Voronezh, Russian Federation).

<https://orcid.org/0000-0003-1658-5579>
ivkov@phys.vsu.ru

Evelina P. Domashevskaya, Dr. Sci. (Phys.–Math.), Full Professor, Department of Solid State Physics and Nanostructures, Voronezh State University (Voronezh, Russian Federation).

<https://orcid.org/0000-0002-6354-4799>
fft@phys.vsu.ru

Received 27.10.2023; approved after reviewing 18.11.2023; accepted for publication 25.12.2023; published online 25.03.2023.

Translated by Vera Frolova